

Bipolar Doping and Band-Gap Anomalies in Delafossite Transparent Conductive Oxides

Xiliang Nie, Su-Huai Wei, and S. B. Zhang

National Renewable Energy Laboratory, Golden, Colorado 80401

(Received 25 September 2001; published 28 January 2002)

Doping wide-gap materials *p* type is highly desirable but often difficult. This makes the recent discovery of *p*-type delafossite oxides, $\text{CuM}^{\text{III}}\text{O}_2$, very attractive. The $\text{CuM}^{\text{III}}\text{O}_2$ also show unique and unexplained physical properties: Increasing band gap from $\text{M}^{\text{III}} = \text{Al, Ga}$, to In , not seen in conventional semiconductors. The largest gap CuInO_2 can be mysteriously doped both *n* and *p* type but not the smaller gaps CuAlO_2 and CuGaO_2 . Here, we show that both properties are results of a large disparity between the fundamental gap and the apparent optical gap, a finding that could lead to a breakthrough in the study of bipolarly dopable wide-gap semiconductor oxides.

DOI: 10.1103/PhysRevLett.88.066405

PACS numbers: 71.20.-b, 78.20.-e

Wide-gap semiconductors are difficult to dope, particularly *p* type. Bipolar doping, namely both *p*- and *n*-type doping, is even more difficult. For example, GaN can be doped *n* type to $5 \times 10^{19} \text{ cm}^{-3}$ electrons but until recently *p*-type doping has been hard to obtain [1,2]. Transparent conducting oxides (TCOs) are another example [3]. These materials, such as ZnO and SnO_2 , have some very unusual physical properties: transparent similar to a glass but conductive almost like a metal. The traditional TCOs can be readily doped *n*-type, to a free-electron level of 10^{21} cm^{-3} , but never *p* type. The one exception is diamond which can, however, only be doped *p* type [4]. Studies [5,6] on these “doping limits” reveal that these seemingly unrelated observations may be related to equilibrium self-compensation by intrinsic defects or solubility issues. More recently, efforts have been devoted to developing *p*-type wide-gap materials and *n*-type diamond using low-*T* [7], nonequilibrium [8], or surface processes [9] to avoid self-compensation while enhancing dopant solubility. As such, the recent discovery [10] of *p*-type delafossite oxide thin films is an important step forward not only because they break ranks with the traditional all *n*-type TCOs, but also because, as we will show below, they provide a mechanism for equilibrium bipolar doping without self-compensation.

Besides showing *p*-type or bipolar conductivity, the $\text{CuM}^{\text{III}}\text{O}_2$ delafossite oxides where $\text{M}^{\text{III}} = \text{Al, Ga, and In}$, also show band-gap anomalies: the optically measured direct band gap increases from 3.5 eV (CuAlO_2) [10,11] to 3.6 eV (CuGaO_2) [12], and to 3.9 eV (CuInO_2) [13]. This trend is in sharp contrast to the trend found in other group-III containing semiconductors. For example, the direct band gap of CuAlS_2 (3.49 eV), CuGaS_2 (2.43 eV), and CuInS_2 (1.53 eV) [14] decreases when the atomic number of the group-III elements increases, as does the direct band gap of AlAs (3.1 eV), GaAs (1.52 eV), and InAs (0.42 eV) [14]. Furthermore, bipolar doping is achieved but only in CuInO_2 by extrinsic dopants [13]. This is quite puzzling because CuInO_2 has the largest reported band gap of 3.9 eV. No similar trend has ever been observed in any other semiconductors.

Using first-principles methods, we have calculated the electronic and optical properties of $\text{CuM}^{\text{III}}\text{O}_2$. We find that while all the materials have indirect band gap, the fundamental direct gap (i.e., the smallest direct band gap) decreases from CuAlO_2 to CuGaO_2 , and to CuInO_2 . In other words, they do follow the general trend of group III containing semiconductors. However, the corresponding dipolar optical transition matrix element at Γ is exactly zero because the two band-edge states have the same (even) parity. An important consequence is that absorption near the fundamental gap at Γ for CuGaO_2 and CuInO_2 is very small and barely increases with energy until transitions at the next critical points take place (which defines an apparent optical band gap). The calculated apparent gap is very much unchanged from CuAlO_2 to CuGaO_2 , but increases by +0.4 eV from CuAlO_2 to CuInO_2 , in good agreement with experiment [10–13]. The large differences in terms of the energy and transition matrix element between the fundamental direct gap and the apparent gap are the reason for the band-gap anomalies seen in $\text{CuM}^{\text{III}}\text{O}_2$. On the other hand, the conduction band minimum (CBM) of CuInO_2 is significantly lower than CuAlO_2 by 1.48 eV. According to the “doping limit rule” [5,6], lower CBM for CuInO_2 implies good *n*-type dopability. Thus a low CBM combined with a large apparent gap explains the puzzling combination of good transparency with bipolar dopability in CuInO_2 .

The calculations were performed using local density approximation (LDA) [15] as implemented by the general potential linearized augmented plane wave (LAPW) method [16]. No shape approximation was used for either the potential or the charge density. We used muffin-tin radii of 2.2, 2.0, and 1.4 bohrs for the group-III atoms, Cu, and O, respectively. The plane wave basis set cutoff energy is 33 Ry. The Ga 3*d* and In 4*d* states are treated as valence states. The lattice parameters *a* and *c*, and the internal parameter *u* are determined by total energy calculation, fitting to the Murnaghan’s equation of state [17]. The Brillouin-zone (BZ) integrations were performed using a $4 \times 4 \times 4$ grid of special **k** points [18]. The optical properties were calculated using the optical package [19] in

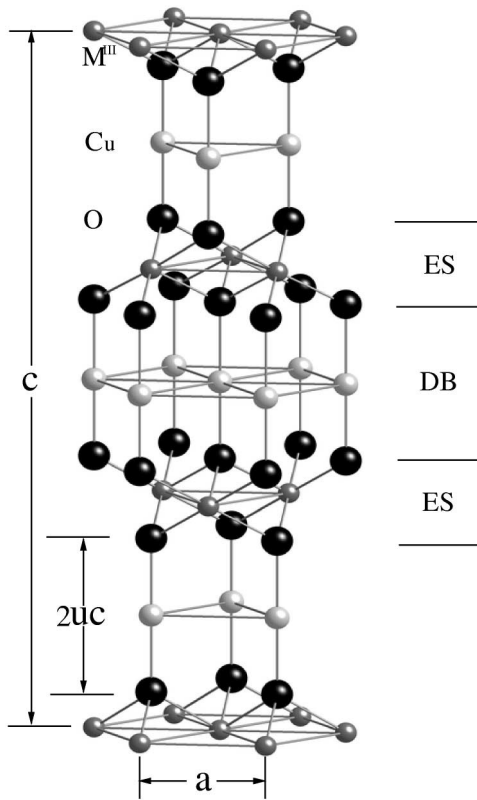


FIG. 1. The crystal structure of delafossite compounds $\text{CuM}^{\text{III}}\text{O}_2$. DB stands for the dumbbell layers and ES stands for the edge-sharing layers.

WIEN97 [20]. The natural valence band offsets are calculated following the same procedure used in photoemission core level spectroscopy as described in Ref. [21].

$\text{CuM}^{\text{III}}\text{O}_2$ have a layered delafossite crystal structure with the space group of $R\bar{3}m$. It is composed of O-Cu-O

TABLE I. Calculated structural parameters for $\text{CuM}^{\text{III}}\text{O}_2$ ($\text{M}^{\text{III}} = \text{Al, Ga, In}$), compared with available experimental data (in parentheses).

	CuAlO_2	CuGaO_2	CuInO_2
a (Å)	2.816 (2.858)	2.963 (2.980)	3.285 (3.292)
c (Å)	16.978 (16.958)	17.172 (17.100)	17.270 (17.388)
u	0.1091 (0.1099)	0.1073	0.1056

dumbbell layers in a hexagonal plane separated by an $\text{M}^{\text{III}}\text{O}_6$ edge-sharing octahedra layer (see Fig. 1). Table I compares the calculated lattice parameters with available experimental values.

The calculated band structures at experimental lattice constants for $\text{CuM}^{\text{III}}\text{O}_2$ are shown in Fig. 2. It is well known that LDA underestimates the band gap. However, in this study, we focus on the difference between the gaps in a group of similar compounds; the systematic LDA error is expected to be largely canceled. The following general trends are observed:

(i) All three compounds have indirect fundamental band gap with the CBM at Γ and the valence band maximum (VBM) on the Γ -F line near F as indicated by the black circles in Fig. 2. The calculated indirect gaps are 1.97, 0.95, and 0.41 eV, respectively, for CuAlO_2 , CuGaO_2 , and CuInO_2 .

(ii) The direct band gap at Γ decreases considerably from 2.93 for CuAlO_2 , to 1.63 for CuGaO_2 , to 0.73 for CuInO_2 . It also decreases at Z from 4.32 to 3.12 to 1.89 eV. This is consistent with the trend in other group-III containing semiconductors. The decrease of the band gap from Al to Ga to In is mainly an atomic size effect: the CBM states at Γ_{1c} and Z_{1c} (or Z_{5c}) have significant antibonding s character. As the volume increases from the Al to

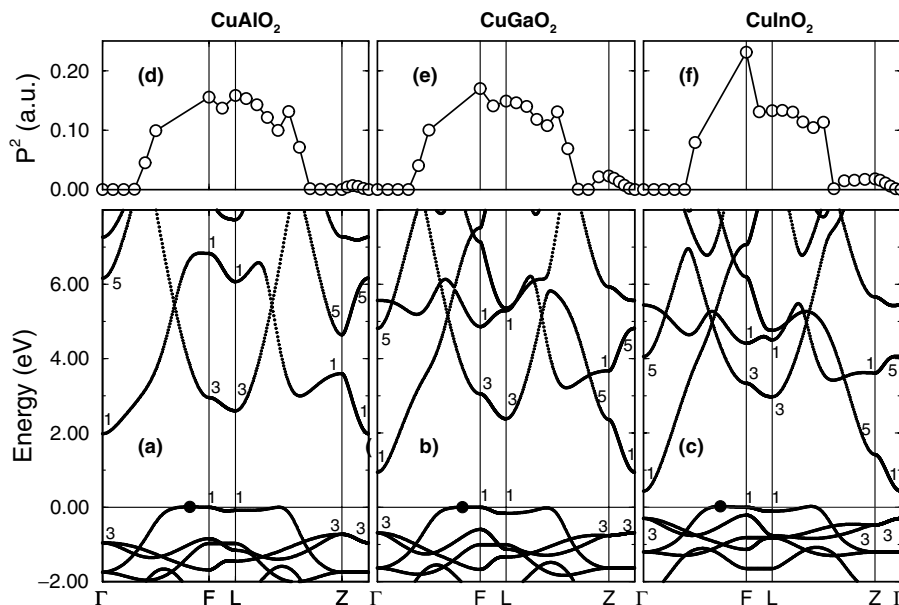


FIG. 2. (a) to (c) are the calculated LDA band structures for CuAlO_2 , CuGaO_2 , and CuInO_2 , respectively. Energy zero is at the highest valence band at F. The VBMs appeared off F are marked by the black circles. (d) to (f) are the corresponding transition matrix elements between the band edge states.

Ga to In compounds, the energies of the antibonding states are lowered. Another contributing factor is the shift of the valence band edge states (Γ_{3v} and Z_{3v}) due to the coupling between the d orbitals of the group-III atoms and the O p orbital. Because Al does not have any occupied d states below the VBM, the VBM of CuAlO_2 at Γ is lower in energy than that of CuGaO_2 and CuInO_2 (see below).

(iii) The direct band gap at F increases from 2.95 for CuAlO_2 , to 3.05 for CuGaO_2 , and to 3.34 for CuInO_2 . A similar trend is observed at L: it decreases slightly from 2.68 for CuAlO_2 to 2.54 for CuGaO_2 , then increases to 3.08 eV for CuInO_2 . The increase of the gap at F (L) from Al or Ga to In is also a size effect. The conduction band edge states F_{3c} and L_{3c} have most of their charge densities in the interstitial region (similar to the X_{1c} and X_{3c} states in the zinc-blende compounds with a negative pressure coefficient). Thus when the volume increases, the energy levels of F_{3c} and L_{3c} also increase. The slight decrease at L from CuAlO_2 to CuGaO_2 is an exception but can be explained in terms of the fact that L_{3c} contains group-III s character and that Ga $4s$ has much lower energy than Al $3s$ orbital.

(iv) For CuGaO_2 and CuInO_2 , the fundamental direct band gap is at Γ . For CuAlO_2 , previous calculation by Yanagi *et al.* [11] suggested that this fundamental direct gap is also at Γ . However, our calculation shows that it is at L instead.

The experimentally observed optical gaps increase from 3.5 (CuAlO_2) [11] to 3.6 (CuGaO_2) [12] to 3.9 eV (CuInO_2) [13]. This trend clearly contradicts the trend in the calculated fundamental direct gaps of 2.68 eV (L) for CuAlO_2 , 1.64 eV (Γ) for CuGaO_2 , and 0.73 eV (Γ) for CuInO_2 , showing a decrease. To resolve this discrepancy, we have calculated the matrix elements for direct transitions between band edge states. The upper panels of Fig. 2 show the results for CuAlO_2 , CuGaO_2 , and CuInO_2 at the Γ , F, L, and Z points and in between. It reveals that direct transitions between Γ_{3v} and Γ_{1c} , and between Z_{3v} and Z_{1c} , are forbidden in the delafossite structure because both states have the same (even) parity [22]. It further suggests that for CuGaO_2 and CuInO_2 the absorption edges increase slowly with energy in the vicinity of the fundamental direct gap at Γ . A sharp increase takes place only when the photon energy is close to the direct transition at F and L.

Indeed, the calculated absorption spectra $\alpha(h\nu)$ in Fig. 3 show very small tails below the abrupt absorption edges for CuGaO_2 and CuInO_2 . In addition, the absorption is highly anisotropic for light perpendicular (\perp) or parallel (\parallel) to the c axis. For the absorption to be effective in TCO thin films, α should satisfy $\alpha l \geq 1$ where l is the thickness of the film. Using the experimental value of $l \sim 300$ nm [10,12,13], we determined the upper bounds on α for transparency to be about $3 \times 10^4 \text{ cm}^{-1}$, much larger than the tail states in Fig. 3. Therefore, the inability to absorb at the fundamental direct gaps in these

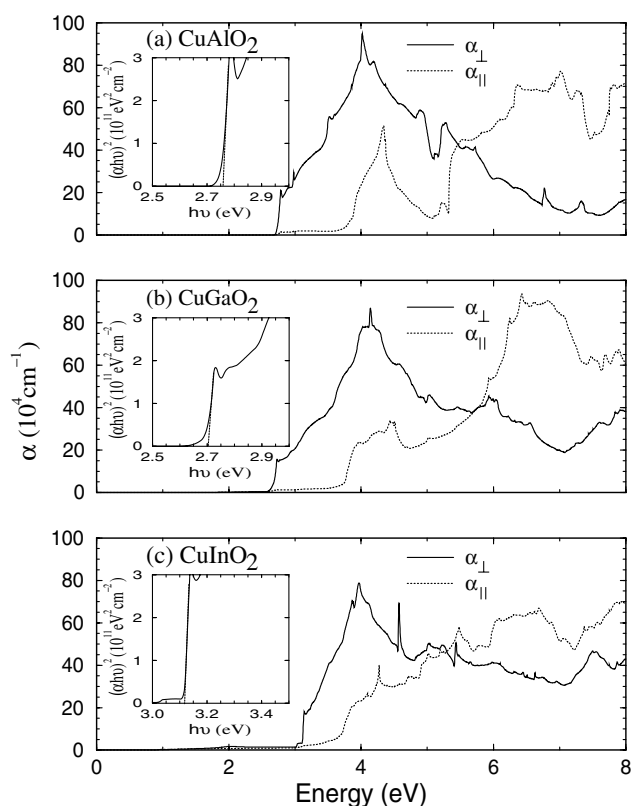


FIG. 3. Calculated LDA dipolar optical absorption spectra for (a) CuAlO_2 , (b) CuGaO_2 , and (c) CuInO_2 . α_{\parallel} and α_{\perp} are for lights parallel and perpendicular to the c axis, respectively. The insets show the $(\alpha h\nu)^2$ vs $h\nu$ plots from which the apparent direct gaps are determined.

materials holds the key for their unusually high thin-film transparency.

To calculate the apparent direct band gap, we have calculated the $(\alpha h\nu)^2$ vs $h\nu$ curves shown as insets in Fig. 3. The LDA values are 2.75, 2.70, and 3.12 eV for CuAlO_2 , CuGaO_2 , and CuInO_2 , respectively. They are systematically smaller than the experimental values of 3.5, 3.6, and 3.9 eV by a constant of about 0.8 eV. This is a typical LDA error. However, the changes of the apparent direct band gaps are in good agreement with experiment. The experimentally observed band gap variation from Al to Ga to In can thus be explained by the change of the apparent direct band gap.

The p -type conductivity of $\text{CuM}^{\text{III}}\text{O}_2$ and the mysterious bipolar dopability of CuInO_2 can also be understood within the framework of equilibrium doping theory. According to the recently developed “doping limit rule” [5,6], the degree of self-compensation in a material correlates directly to its band-edge positions with respect to others. A compound with higher VBM is easier to dope p type, while a compound with lower CBM is easier to dope n type. Because Cu has a much shallower $3d$ orbital than Zn, coupling between the Cu $3d$ and O $2p$ states will push up the VBM of $\text{CuM}^{\text{III}}\text{O}_2$ with respect to ZnO, leading to better p -type conductivity. Our calculated result shows that the VBM for CuGaO_2 is indeed 0.8 eV higher than ZnO, as

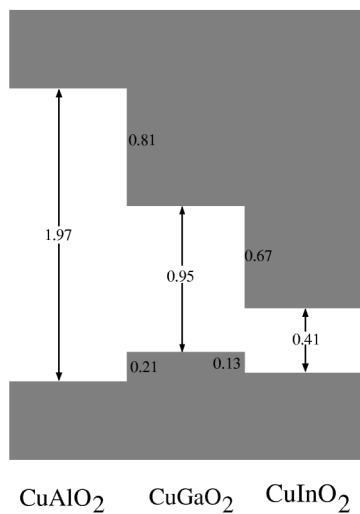


FIG. 4. Calculated LDA band alignments between CuAlO_2 , CuGaO_2 , and CuInO_2 .

expected. Furthermore, the antibonding p - d character [23] at the VBM makes the formation of the Cu vacancy much easier in $\text{CuM}^{\text{III}}\text{O}_2$, thus enhancing their p -type dopability. We have calculated the formation energies for a number of important defects in p -type CuGaO_2 with the Fermi energy at the VBM: the Cu vacancy (V_{Cu}) which is known to be a shallow acceptor, the oxygen vacancy (V_{O}), and Cu interstitial (Cu_i) that may cause self-compensation to acceptors. At the Cu-rich condition, $\Delta H_f(V_{\text{Cu}}^-)$ is about 4.5 eV lower than $\Delta H_f(V_{\text{Zn}}^{2-})$ in ZnO at the Zn-rich condition [24]. But $\Delta H_f(\text{Cu}_i^+)$ is about 2 eV higher than $\Delta H_f(\text{Zn}_i^{2+})$. For oxygen vacancy, the compact delafossite structure limits lattice relaxation so V_{O} does not ionize in $\text{CuM}^{\text{III}}\text{O}_2$. At the O-rich condition, $\Delta H_f(V_{\text{O}}^0)$ is about 4 eV higher than $\Delta H_f(V_{\text{O}}^0)$ in ZnO. A great reduction in self-compensation plus lower acceptor formation energy, thus, explains why $\text{CuM}^{\text{III}}\text{O}_2$ is p type and reinforces the “doping limit rule.”

Figure 4 shows the calculated band alignments among $\text{CuM}^{\text{III}}\text{O}_2$. The valence band offsets for this common-anion system are rather small. The slightly higher VBMs for CuGaO_2 and CuInO_2 than for CuAlO_2 are a result of the coupling between the group-III d orbitals and the O p orbital. Hence, p -type conductivity might be slightly easier to reach in CuGaO_2 and CuInO_2 than in CuAlO_2 . On the other hand, due to a large volume deformation, the CBM of CuInO_2 is 1.48 eV lower than CuAlO_2 . This explains why n -type conductivity can also be achieved in this nominally p -type material.

In summary, first-principles calculations resolve the mysteries surrounding p -type $\text{CuM}^{\text{III}}\text{O}_2$ ($\text{M}^{\text{III}} = \text{Al}, \text{Ga}, \text{In}$). We found that the fundamental direct band gap decreases from Al to Ga to In, but the apparent optical band gap of CuInO_2 is about 0.4 eV higher than that of CuAlO_2 , in good agreement with experiment. This explains the band-gap anomalies observed in these

systems. More importantly, our calculations explain the p -type conductivity in $\text{CuM}^{\text{III}}\text{O}_2$, and the unusual bipolar dopability observed in CuInO_2 by the exceptionally large disparity between its fundamental indirect band gap and apparent direct band gap. This finding sheds new light on the search for bipolarly dopable transparent conductive oxides and on doping wide-gap materials in general.

We thank Tihu Wang for illuminating discussions. This work was supported by the U.S. DOE-SC-BES under Contract No. DE-AC36-99GO10337.

- [1] S. Nakamura, M. Senoh, and N. Iwasa, *Jpn. J. Appl. Phys.* **31**, L139 (1992).
- [2] J. Nengebauer and C. G. Van de Walle, *Phys. Rev. Lett.* **75**, 4452 (1995).
- [3] See *Rev. MRS Bull.* **25**, No. 8 (2000).
- [4] S. Koizumi *et al.*, *Science* **292**, 1899 (2001).
- [5] S. B. Zhang, S.-H. Wei, and A. Zunger, *J. Appl. Phys.* **83**, 3192 (1998).
- [6] S. B. Zhang, S.-H. Wei, and A. Zunger, *Phys. Rev. Lett.* **84**, 1232 (2000).
- [7] M. Joseph, H. Tabata, and T. Kawai, *Jpn. J. Appl. Phys.* **38**, L1205 (1999).
- [8] Y. Yan, S. B. Zhang, and S. T. Pantelides, *Phys. Rev. Lett.* **86**, 5723 (2001).
- [9] S. B. Zhang and S.-H. Wei, *Phys. Rev. Lett.* **86**, 1789 (2001).
- [10] H. Kawazoe *et al.*, *Nature (London)* **389**, 939 (1997).
- [11] H. Yanagi *et al.*, *J. Appl. Phys.* **88**, 4159 (2000).
- [12] K. Ueda, T. Hase, H. Yanagi, H. Kawazoe, H. Hosono, H. Ohta, M. Orita, and M. Hirano, *J. Appl. Phys.* **89**, 1790 (2001).
- [13] H. Yanagi, T. Hase, S. Ibuki, K. Ueda, and H. Hosono, *Appl. Phys. Lett.* **78**, 1583 (2001).
- [14] *Landolt-Bornstein: Numerical Data and Functional Relationships in Science and Technology*, edited by O. Madelung and M. Schulz (Springer-Verlag, Berlin, 1987), Group III, Vol. 22a.
- [15] P. Hohenberg and W. Kohn, *Phys. Rev.* **136**, B864 (1964); W. Kohn and L. J. Sham, *ibid.* **140**, A1133 (1965).
- [16] S.-H. Wei and Krakauer, *Phys. Rev. Lett.* **55**, 1200 (1985); D. J. Singh, *Planewaves, Pseudopotentials and the LAPW Method* (Kluwer, Boston, 1994).
- [17] F. D. Murnaghan, *Proc. Natl. Acad. Sci. U.S.A.* **30**, 244 (1944).
- [18] H. J. Monkhorst and J. P. Pack, *Phys. Rev. B* **13**, 5188 (1976).
- [19] R. Abt, C. Ambrosch-Draxl, and P. Knoll, *Physica (Amsterdam)* **194B–196B**, 1451 (1994).
- [20] P. Blaha, K. Schwarz, P. Sorantin, and S. B. Trickey, *Comput. Phys. Commun.* **59**, 399 (1990).
- [21] S.-H. Wei and A. Zunger, *Appl. Phys. Lett.* **72**, 2011 (1998).
- [22] P. Y. Yu and M. Cardona, *Fundamentals of Semiconductors* (Springer-Verlag, Berlin, 1996).
- [23] S. B. Zhang, S.-H. Wei, A. Zunger, and H. Katayama-Yoshida, *Phys. Rev. B* **57**, 9642 (1998).
- [24] S. B. Zhang, S.-H. Wei, and A. Zunger, *Phys. Rev. B* **63**, 75205 (2001).